A catalytic reactor for the trapping of free radicals from gas phase oxidation reactions

Marco Conte, Karen Wilson, and Victor Chechik

Citation: Review of Scientific Instruments **81**, 104102 (2010); doi: 10.1063/1.3492247
View online: https://doi.org/10.1063/1.3492247
View Table of Contents: http://aip.scitation.org/toc/rsi/81/10
Published by the American Institute of Physics

A catalytic reactor for the trapping of free radicals from gas phase oxidation reactions

Marco Conte,[1,2,a)] Karen Wilson,[1,2] and Victor Chechik[1]
[1]*Department of Chemistry, University of York, Heslington, York, YO10 5DD, United Kingdom*
[2]*Cardiff Catalysis Institute, Cardiff University, Cardiff, CF10 3AT, United Kingdom*

(Received 6 July 2010; accepted 24 August 2010; published online 20 October 2010)

A catalytic reactor for the trapping of free radicals originating from gas phase catalytic reactions is described and discussed. Radical trapping and identification were initially carried out using a known radical generator such as dicumyl peroxide. The trapping of radicals was further demonstrated by investigating genuine radical oxidation processes, e.g., benzaldehyde oxidation over manganese and cobalt salts. The efficiency of the reactor was finally proven by the partial oxidation of cyclohexane over MoO_3, Cr_2O_3, and WO_3, which allowed the identification of all the radical intermediates responsible for the formation of the products cyclohexanol and cyclohexanone. Assignment of the trapped radicals was carried out using spin trapping technique and *X*-band electron paramagnetic resonance spectroscopy. © *2010 American Institute of Physics.* [doi:10.1063/1.3492247]

I. INTRODUCTION

Gas phase radicals play an important role in many chemical processes such as atmospheric chemistry,[1] combustion of organic materials,[2] and gas phase catalytic oxidation reactions.[3] However, investigations of these processes are limited by the need to efficiently capture the radicals before termination or radical quenching occurs, as well as the availability of a suitable method to identify the radicals trapped. Identification of radical species can be conveniently carried out using electron paramagnetic resonance (EPR) spectroscopy.[4] However, direct application of EPR to gas phase species is precluded due to spin-rotational coupling.[5] This limitation can be overcome making use of matrix isolation techniques[6] or spin trapping methods.[7]

The matrix isolation method relies on the collection of gaseous effluents in an inert hydrocarbon matrix (usually isopentane) or CO_2 cooled at liquid nitrogen temperature (77 K). The sample is then analyzed via conventional EPR spectroscopy. This method has been applied to atmospheric analysis[8] or single atoms detection studies.[9] However, this form of analysis is extremely difficult because it relies on efficient concentration of the sample from the gas phase to the solid phase, and prolonged radical life time at low temperatures, limiting the practical applicability of this method.

By contrast, the spin trapping methodology relies on the fast selective addition (trapping) of short-lived radicals to a diamagnetic spin trap, usually a nitrone or a nitroso compound, such as 5,5-dimethyl-1-pyrroline-N-oxide (DMPO). The product of this addition (spin adduct) is a persistent free radical (nitroxide) with sufficiently long lifetime, usually up to tens of minutes, which enables detection by conventional EPR spectroscopy (Fig. 1) in the *X*-band (8–12 GHz). This approach has been extensively used in liquid phase for biological samples,[10] and it found applications in reaction mechanism studies,[11,12] and catalysis in liquid phase.[13,14] At present the use of spin trapping methods for gas phase systems is limited to the wood or tobacco industry,[15,16] and it has never been applied to gas phase catalytic reactions.

The reason for this is that spin trap molecules are unstable at the temperatures usually required for heterogeneous gas phase reactions (generally above 150 °C). Moreover, under these conditions, the spin adducts can undergo structural rearrangements, which can lead to ambiguity or difficulty assigning the structure of the original free radical trapped by the spin trap molecule.[17]

To overcome these limitations, here we describe the design, construction, and application of a reactor for the capture of radicals formed in the gas phase catalytic reactions, making use of a tubular fixed bed reactor. In this setup, the reactor effluents were rapidly cooled to room temperature immediately after leaving the catalytic bed, and collected in a toluene solution containing a spin trap, which was then analyzed by conventional *X*-band EPR spectroscopy.

We report on the design of a reactor and methodology, which allows the trapping and identification of short-lived radical species that cannot be detected by conventional methods. This new approach also allows an estimation of the lifetime of these radical species, and it could be helpful in the clarification of reaction mechanisms involving peroxides over metal oxides surfaces.[18] Preliminary studies using dicumyl peroxide (DCP) and benzaldehyde were employed to validate the reaction, after which it was employed to trap radicals formed during the industrially relevant gas phase oxidation of cyclohexane over metal oxides[19] such as MoO_3, Cr_2O_3, and WO_3.

II. EXPERIMENTAL

A. Reactor design

A schematic diagram of the gas phase reactor employed to capture the radicals generated from the gas phase reaction

a)Author to whom correspondence should be addressed. Electronic mail: conteM1@cardiff.ac.uk.

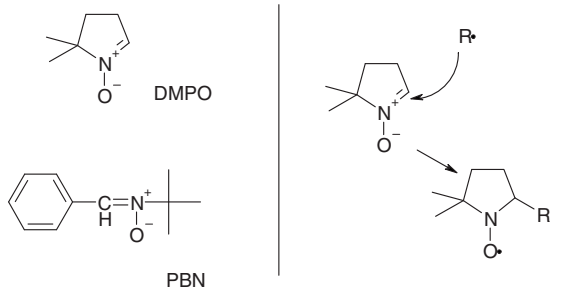

FIG. 1. Chemical structure of DMPO and PBN spin traps (left) and trapping of a free radical (right).

is shown in Fig. 2. The reactor was built by a stainless steel tube 105 mm long with internal diameter of 4.83 mm [Swagelock outer diameter (OD) 1/4 in.]. A catalytic bed of the metal oxide (20 mg) or the radical generator (typically 5 mg) was placed at the bottom of the tube, supported by a silica wool layer standing on a metal grid in order to avoid any transfer of the metal oxide to the spin trapping solution. The reactor was heated using a heating tape allowing an operational temperature range from 50 to 300 °C. The temperature used to carry out the experiments was typically 180 °C. In order to increase the linear velocity of the effluents, and to reduce the dead volumes, the bottom of the catalytic bed was monolithically joined to a tube with an internal diameter of 2.23 mm (Swagelock OD 1/8 in.). The reactor was fed from the top via a saturator containing the substrate under N_2 or air flow.

The main features of the system are designed to achieve a fast transfer of the radicals from the catalytic bed to the spin trapping solution, as well as to obtain immediate cooling of the reactor effluents. The feed gas was initially controlled by means of a flow meter (Brooks Sho-Rate 1355), which allowed a flow from 0 to 100 ml/min. For higher values, up to 1000 ml/min, an electronic thermal mass flow controller (Brooks Smart Mass Flow-Flotech 5850 S) with an inlet pressure of 2 bar was used. Cooling of the reactor effluents in the narrower section after the catalytic bed was achieved using a brass heat exchanger (size: 60 mm diameter

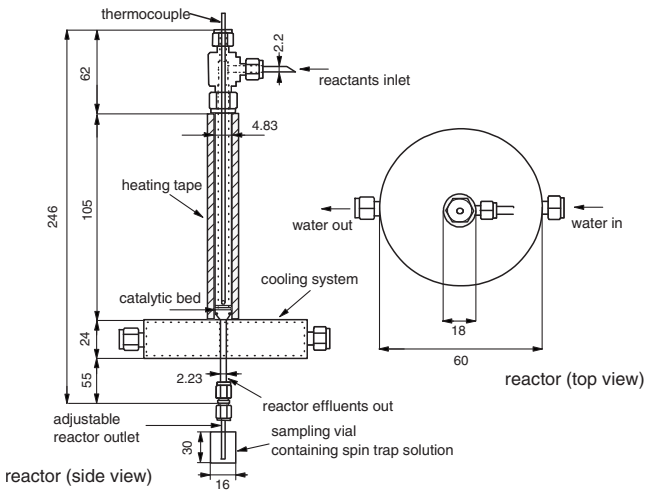

FIG. 2. Schematic diagram of the spin trapping reactor (sizes quoted in millimeter).

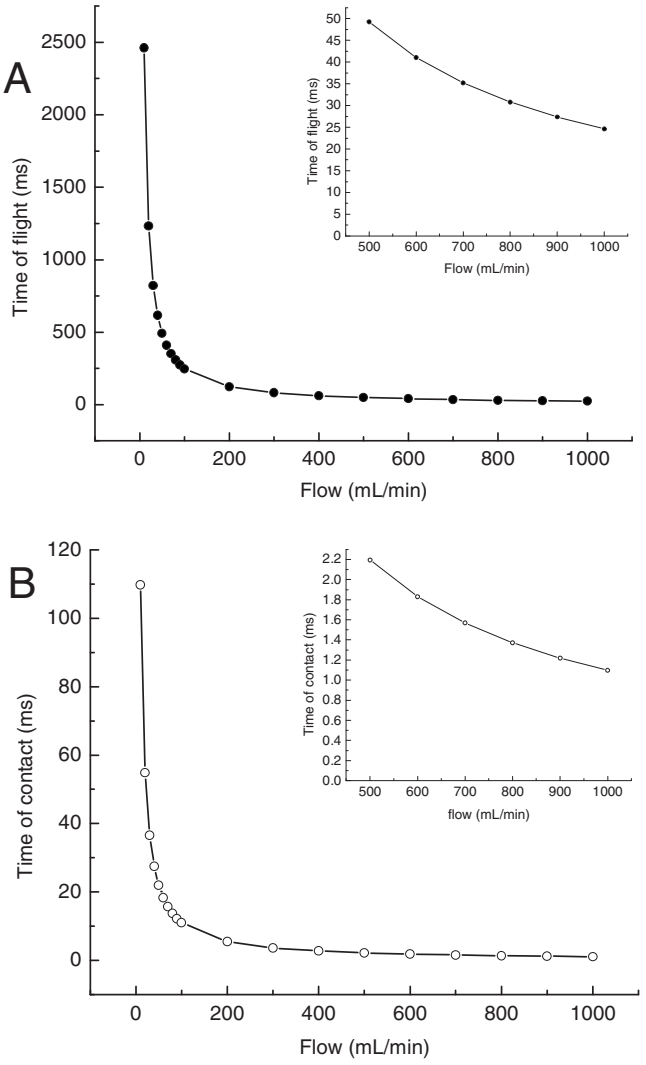

FIG. 3. (a) Time of flight of the reactor effluents vs flow rate for a standard 5 cm (2.23 mm ID) pathway from the catalytic bed to the spin trapping solution. (b) Time of contact vs flow rate of the reactants over the catalytic bed (4.83 mm OD×1 mm bed thickness).

and 24 mm deep) fed with cold water at 7 °C. This cooled the reactor effluents from 180 to 22 °C even at 1000 ml/min flow rate. The reactor outlet was then joined to a PTFE tube (the standard tests were carried out on a Swagelock OD 1/8 in. Internal diameter (ID) 2.23 mm which had the same dimensional values of the stainless steel) immersed in a toluene/DMPO solution for 20–40 min contained in a vial 30 mm deep and 16 mm of diameter. The solution was then concentrated and analyzed via *X*-band EPR spectroscopy. Using these dimensional values, it is possible to calculate the time of flight of the radical species from the catalytic bed to the spin trapping solution [Fig. 3(a)] and in the case of cyclohexane oxidation, the time of contact of the substrate with the catalytic bed [Fig. 3(b)]. If the reactor is used at its higher flow rate (1000 ml/min), these time values lie in the range of ca. 25 and 1.2 ms for the time of flight and the time of contact, respectively.

B. EPR and spin trapping experiments

X-band EPR spectra were recorded at room temperature, using a Bruker ESP-300 E spectrometer. The typical instru-

ment parameters were as follows: center field 3485 G, sweep width 100 G, sweep time 82 s, time constant 20 ms, power 5 mW, modulation frequency 100 kHz, and modulation width 0.97 G. Quantitative spectral analysis was carried out using WINSIM software.[20] The reactor effluents were collected in a DMPO/toluene solution (50 μL of DMPO in 2 ml of toluene). Collection of the reactor effluents was carried out up to total consumption of the substrate in the saturator (23 min were required when cyclohexane was used, with the saturator heated at 40 °C and inlet flow of Air or N_2 of 1000 ml/min). The resulting solution was then concentrated using a rotary evaporator to a final volume of 200 μl, transferred into a glass tube and deoxygenated by bubbling nitrogen for ca. 1 min before recording the EPR spectra. Using such experimental conditions, the overall intensities of the spectra was comparable to a $10^{-4}M$ 2,2,6,6-tetramethyl-piperidine-1-oxyl (TEMPO) solution used as standard.

DMPO, N-tert-butyl-α-phenylnitrone (PBN), toluene, MoO_3, Cr_2O_3, and WO_3, were purchased by Aldrich (ACS reagents purity grade) and used without any further treatment. The use of toluene in the spin trapping solution was due to its lower volatility.

C. Gas chromatographic analysis of the reactor effluents

To emulate the spin trapping reaction conditions, MoO_3 (20 mg) was used, using a reaction temperature of 180 °C and an air inlet flow of 1000 ml/min. The reactor was fed with 4 ml of cyclohexane through a saturator heated at 40 °C. The reactor effluents were condensed and collected in a cold trap at 0 °C. The reaction mixture was analyzed via gas chromatography using a Shimadzu gas-chromatograph with an initial column temperature of 50 °C and a final column temperature of 350 °C. The temperature ramp was 5 °C/min and the final temperature was held for 20 min. Injector and detector temperatures were both 350 °C. A chromatographic column Zebron ZB-5 (30 m length, 0.25 mm ID, and 0.25 μm film thickness) was used.

III. RESULTS AND DISCUSSION

The feasibility and efficiency of the reactor were first tested by trapping radicals from DCP decomposition, and benzaldehyde and cyclohexane oxidation.

A. Trapping of radicals from thermal DCP decomposition

DCP is known to undergo homolytic decomposition above 100 °C with a half life of 0.3 h at 145 °C.[21] The resulting cumyloxyl radical can further decompose to acetophenone and methyl radicals.[22] The cumyloxyl radical can also decompose to α-methyl styrene following hydrogen abstraction from a suitable substrate (Scheme 1).

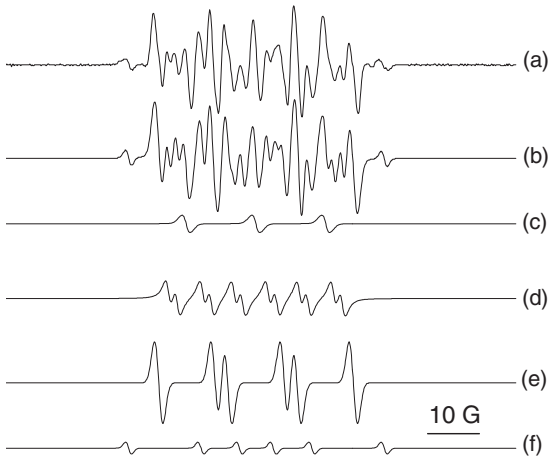

FIG. 4. EPR spectrum deconvolution of the spin adducts obtained during the thermal DCP decomposition at 140 °C and 100 ml of N_2 inlet flow using DMPO as spin trap. (a) Experimental spectrum, (b) simulated spectrum, (c) di-t-alkyl nitroxide radical, (d) RO· adduct, (e) ROO· adduct, and (f) carbon $Ph(CH_3)_2C$· spin adduct.

Primary DCP decomposition:

$$Ph(CH_3)_2C-O-O-C(CH_3)_2Ph \rightarrow 2Ph(CH_3)_2C-O\cdot$$

Cumyloxyl radical decomposition:

$$Ph(CH_3)_2C-O\cdot \rightarrow PhCOCH_3 + CH_3,$$
$$Ph(CH_3)_2C-O\cdot \rightarrow Ph(CH_3)_2COH \rightarrow PhCH_3C=CH_2 + H_2O.$$

SCHEME 1. Thermal decomposition routes for DCP.

Therefore, it was a good model system to initially test the ability of the reactor to generate and trap radicals. Figure 4(a) shows the EPR spectrum of the trapped effluent following decomposition of 5 mg of DCP at 140 °C under a 100 ml/min flow of nitrogen for 20 min.

Simulation of the spectrum to determine nitrogen (a_N) and proton (a_H) coupling constants [Fig. 4(b)] and comparison with literature values makes it possible to identify the following species [Figs. 4(c)–4(f)]: a weak a di-t-alkyl nitroxide radical (a_N=13.7 G),[23] the clear presence of an alkoxyl RO· adduct (a_N=12.85, $a_{H(\beta)}$=6.70, $a_{H(\gamma)}$=1.71 G),[24] an ROO· adduct (a_N=13.57, a_H=11.06 G),[25] and significantly a carbon centered adduct (a_N=14.21, a_H=21.76 G)[26] consistent with the formation of $Ph(CH_3)_2C$· rather than CH_3· adducts, as the latter are expected to have a_H in the range of 20.5 G.[27]

The presence of peroxyl species could be explained by reaction of the carbon centered radicals with O_2 released by DCP during its decomposition, a reaction which is known to be extremely fast,[28] while the di-t-alkyl nitroxide radical could be due to oxidation of DMPO by the peroxide species.[23] The relative amount of the radicals is calculated

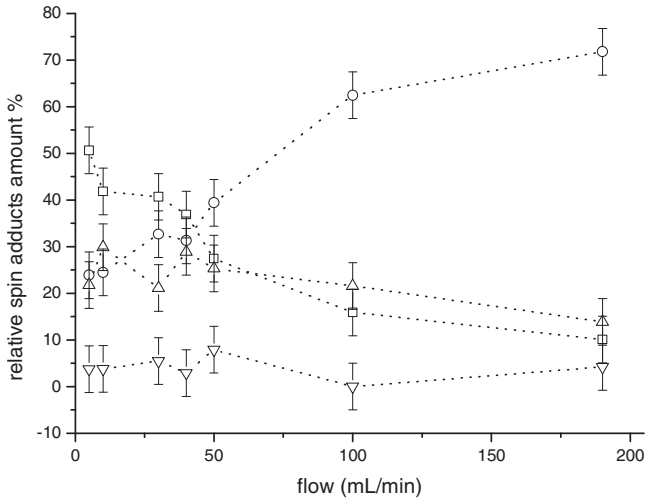

FIG. 5. Relative DMPO spin adducts amount (to 100%) for the DCP decomposition for various N_2 inlet flows. (□) RO· adduct, (○) ROO· adduct, (△) di-t-alkyl nitroxide radical, and (▽) carbon ($Ph(CH_3)_2C$·) spin adduct.

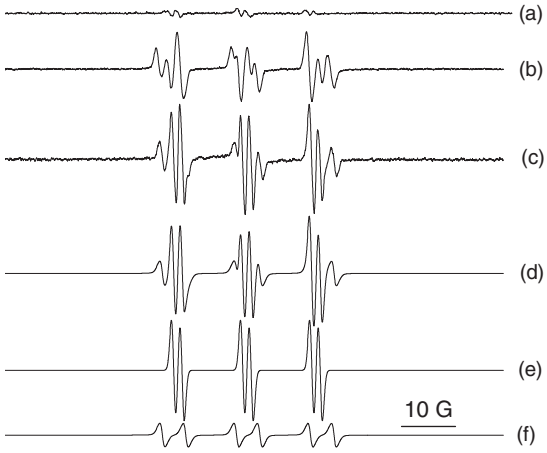

FIG. 6. EPR spectra of the spin adducts obtained during the aerobic oxidation of benzaldehyde in air, using PBN as a spin trap. (a) Benzaldehyde only with empty reactor, (b) reactor containing cobalt acetyl acetonate, (c) reactor containing manganese acetate, (d) simulated spectrum of test c, (e) simulated PhCO—OO·, and (f) PhC·O adducts.

from the intensity of the spin trapping spectra, then by repeating the experiment under different flow conditions, an increase in the relative amount of ROO· radicals is observed relative to the RO· species as the N_2 flow is reduced (Fig. 5). This finding is consistent with the longer lifetimes of peroxyl radicals compared to alkoxyl radicals and verifies the performance of the reactor for trapping short lived radical species.[29]

However, it is also possible to observe that flow rates of nitrogen below 50 ml/min led to scattered measurements with no clear trend. Additionally, EPR signals were only observed if high amount of DCP was used in the tests. The detection limit of EPR methods is usually well below 10^{16} spins.[30] Moreover, no $\cdot CH_3$ spin adduct is detected, likely because it is an extremely reactive radical with short lifetime.

This prompted us to use the higher flow rates of carrier gas to investigate: (i) a catalytic reaction known to proceed via radical pathway and (ii) a catalytic system capable of generating a wide range of radicals in the gas phase, to fully test the performance of the setup in use.

B. Trapping of radicals in the benzaldehyde oxidation over Mn and Co salts

Aldehydes are autoxidized by air via a radical pathway;[31] this reaction is facilitated by manganese, copper, and cobalt salts, which promote the initiation step by generating an acyl radical.[32] This further reacts with oxygen to form peroxyl radicals (Scheme 2). The reaction can then proceed by abstraction of a hydrogen atom from the aldehyde by the peroxyl radical (giving a peracid) during the propagation step, to finally yield the carboxylic acid from the aldehyde and peracid via the Baeyer–Villiger reaction.

Initiation:

$$PhCOH \rightarrow PhC^{\cdot}O.$$

Propagation:

$$PhC^{\cdot}O + O_2 \rightarrow PhCO — OO\cdot$$

$$PhCO — OO\cdot + PhCOH \rightarrow PhCO — OOH + PhC^{\cdot}O.$$

Acid formation:

$$PhCO — OOH + PhCOH \rightarrow 2PhCOOH.$$

SCHEME 2. Benzaldehyde autoxidation pathway to benzoic acid in air. Manganese and cobalt based catalysts promote the initiation step.

For this series, PBN was used as a spin trap, as it is known to lead to very characteristic and diagnostic coupling constants in the presence of acyl radicals (>4 G in the case of benzoyl adducts).[33] If benzaldehyde alone is introduced into the system at 130 °C under an air flow of 300 ml/min, only a weak signal ascribed to peroxyl adducts, RCO—OO·, (a_N=13.36, a_H=1.51 G)[34] is observed [Fig. 6(a)]. In contrast, when the reactor was loaded with 20 mg of cobalt acetyl acetonate [Fig. 6(b)] or manganese acetate [Fig. 6(c)] and the reaction performed at 80 °C, intense signals were detected which allow to clearly identify both peroxyl adducts (a_N=13.36, a_H=1.58 G)[34] and the characteristic benzoyl radical (a_N=14.3, a_H=4.53 G)[33] [simulation and spectra deconvolution are in Figs. 6(d)–6(f)].

This is consistent with the catalytic role of the metals involved. Moreover, the clear presence of benzoyl adducts means that the reactor allows fast detection of the benzoyl species before they can react with the oxygen present in the reaction atmosphere, further proving the feasibility of the setup in use.

C. Trapping of radicals in the cyclohexane oxidation over MoO_3

The selective oxidation of cyclohexane to cyclohexanol and cyclohexanone over metal oxides was also investigated

to assess the versatility of this reactor for trapping radicals formed in heterogeneously initiated oxidation reaction. This reaction has been extensively studied in liquid phase using homogeneous cobalt based catalyst,[35] and in this case, it is ascertained to proceed via a radical route. Heterogeneous partial oxidation in liquid phase is also possible using MoO_3, Cr_2O_3, and WO_3.[36] In the current study, we tested these metal oxides under gas phase conditions, in order to determine the full capability of the reactor. In fact, this reaction is much more challenging and complex to investigate than the previous one as it involves complex multistep reactions, with several intermediate species (Scheme 3).

Initiation:

$$C_6H_{12} \rightarrow C_6H_{11}\cdot$$

Propagation:

$$C_6H_{11}\cdot + O_2 \rightarrow C_6H_{11}\text{—}OO\cdot$$

$$C_6H_{11}\text{—}OO\cdot + C_6H_{12} \rightarrow C_6H_{11}\text{—}OOH + C_6H_{11}\cdot$$

Cyclohexanone formation:

$$C_6H_{11}\text{—}OO\cdot + C_6H_{11}OOH \rightarrow C_6H_{11}OOH + C_6H_{10}(\cdot)OOH$$

$$C_6H_{10}(\cdot)OOH \rightarrow C_6H_{10}{=}O + OH\cdot$$

Cyclohexanol formation:

$$C_6H_{11}\text{—}O\cdot + C_6H_{12} \rightarrow C_6H_{11}\text{—}OH + C_6H_{11}\cdot$$

Peroxyl condensation reaction:

$$2C_6H_{11}\text{—}OO\cdot \rightarrow C_6H_{11}\text{—}OH + C_6H_{10}{=}O + O_2$$

SCHEME 3. Partial oxidation of cyclohexane to cyclohexanol and cyclohexanone in air. The metal oxides catalysts promote the initiation step; they can also be source of oxygen in the final product.

Cyclohexane was fed into the reactor (180 °C) using a saturator with an air flow of 1000 ml/min. Metal oxide (50 mesh, 20 mg) was loaded into the reactor tube to form a catalyst bed of ca. 1 mm thickness. Using these dimensional values a gas hourly space velocity (GHSV) of ca. 3.3×10^9 h^{-1} is obtained, which is 10^4—10^6 times higher than the typical values used in gas phase microreactors to evaluate conversion and selectivity.[37] Low conversion values, less than 0.5%, were determined via gas chromatography for cyclohexanone and cyclohexanol as the only products (with a 1:1 selectivity ratio). On the other hand, this high GHSV is needed to ensure trapping of the radicals, which will not be otherwise detected. It is also worth noting that under such experimental conditions the radical flux is much lower than in the case of DCP decomposition or benzaldehyde oxidation, thus a ~25 times more concentrated DMPO spin trapping solution was employed.

Using MoO_3 as a catalyst and cyclohexane as substrate, the EPR spectra [Fig. 7(a)] show a large number of spin adducts. Simulation of the spectrum [Fig. 7(b)] makes it possible to identify the following species [Figs. 7(c)–7(i)]: the di-t-alkyl nitroxide radical (a_N=14.03),[23] a DMPO oxidation product (a_N=14.42, a_H=2.76 G),[38] an RO· adduct (a_N=12.85, $a_{H(\beta)}$=7.24, $a_{H(\gamma)}$=1.82 G),[24] an ROO· adduct (a_N=13.70, a_H=10.70 G),[25] ·OH (a_N=14.90, a_H=12.31 G),[39] a possible allyl radical (a_N=14.82, a_H=16.08 G),[40] and a carbon centered adduct characteristic of $C_6H_{11}\cdot$ (a_N=13.98, a_H=21.39 G).[41] The observation of these species shows complete consistency with the free radical chain reaction models of cyclohexane oxidation developed in the literature, which yields cyclohexanol and cyclohexanone as main products,[42,43] thus proving in full the feasibility of our experimental setup.

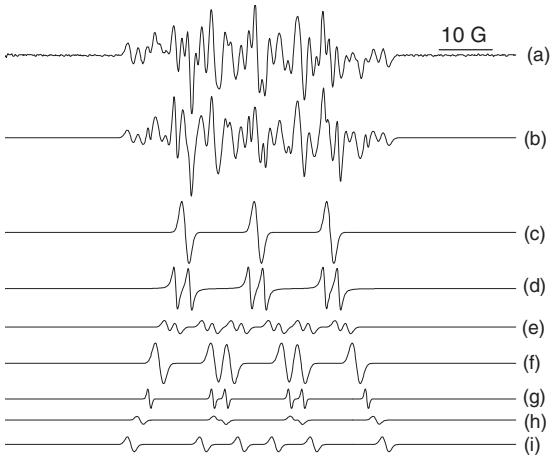

FIG. 7. EPR spectrum deconvolution of the spin adducts obtained during cyclohexane oxidation over MoO_3 at 180 °C in aerobic conditions using DMPO as a spin trap. (a) Experimental spectrum and (b) simulated spectrum. (c) Di-t-alkyl nitroxide radical, (d) DMPO oxidation product, (e) RO· adduct, (f) ROO· adduct, (g) ·OH adduct, (h) possible allyl radical, and (i) the characteristic $C_6H_{11}\cdot$ adduct.

Interestingly, when the length of the reactor outlet was increased to increase the time of flight of the radicals, a clear decrease in the intensity of the spin adducts was detected (Fig. 8). This verifies that the radicals trapped are genuinely obtained by reaction of cyclohexane over MoO_3.

Changing the time of flight of the radicals allowed accurate determination of the lifetime of C_6H_{11}—OO·, C_6H_{11}—O· and $C_6H_{11}\cdot$ radicals in the gas phase (Fig. 9). In

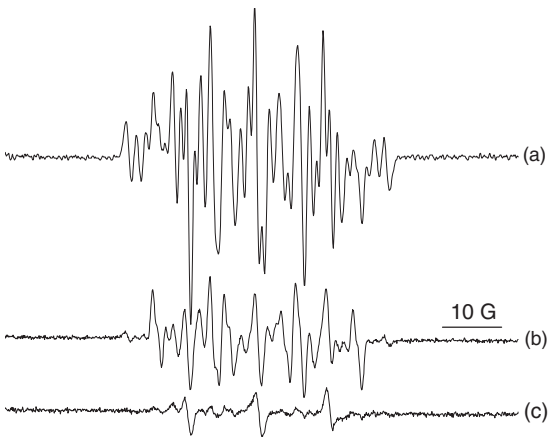

FIG. 8. DMPO spin adducts from the reaction of cyclohexane over MoO_3 at 180 °C in aerobic conditions. Reactor outlets dimensional values as follows: (a) 5 cm × 2.23 mm ID (time of flight 25 ms), (b) 25 cm × 2.23 mm ID (time of flight 62 ms), and (c) 10 cm × 10 mm ID (time of flight 484 ms) (5 cm of the heat exchanger is already included in the time of flight).

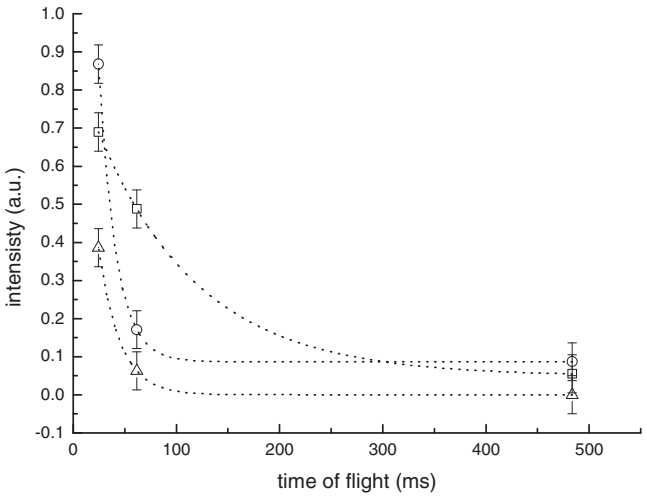

FIG. 9. DMPO spin adducts intensity decay for (□) ROO·, (○) RO·, and (△) C_6H_{11}·.

fact, fitting the intensities of the corresponding spin adducts to a first order rate law led to the following radicals life time, expressed as $t_{1/2}$: ROO·98 ms, RO·17 ms, and C_6H_{11}·20 ms, which are in the range of the expected values for these species.[44]

D. Trapping of radicals in the cyclohexane oxidation over Cr_2O_3, WO_3, and requirements of the catalytic bed

Cr_2O_3 and WO_3 are also known to display reactivity toward cyclohexane oxidation, although with lower efficiency[45] due to reduced lattice oxygen mobility.[46,47] In this case, we observed a simplified spectrum of spin adducts moving from MoO_3 to WO_3 including a reduced overall intensity accompanied by complete disappearance of the parent C_6H_{11}· radical for the latter catalyst, which is considered responsible for the initiation step for this reaction (Fig. 10).

It is worth noting that variations in the catalytic bed thickness led to some apparently counterintuitive results. In fact, excessively large catalytic bed (200 mg) did not lead to any radical detection. We think this behavior is related to the quenching of peroxyl radicals that are the key intermediates for cyclohenanone and cyclohexanol by the metal oxide itself. In fact, all the metal oxides tested present neutral oxygen vacancies[48,49] that could possibly locate peroxyl species. In other words, the catalytic material can act as both initiator (due to the presence of activated surface oxygen) and quencher (due to the presence of oxygen vacancies). This will need to be considered in order to further develop the current experimental setup.

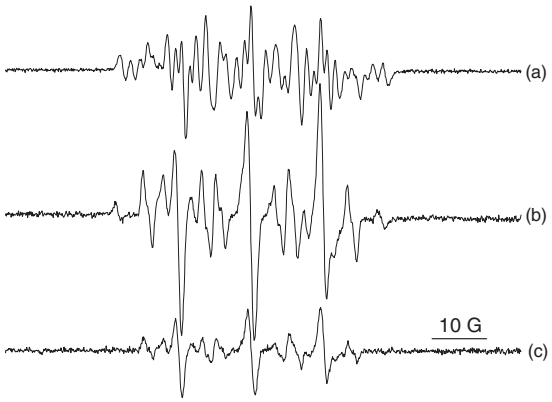

FIG. 10. EPR spectra of spin adducts for the cyclohexane oxidation in air at 180 °C over: (a) MoO_3, (b) Cr_2O_3, and (c) WO_3, using DMPO as spin trap.

IV. CONCLUSIONS

We have developed a new experimental tool for studying gas phase radical reactions using EPR spin trapping methodology combined with a high flow catalytic reactor. The study of model systems such as DCP decomposition and benzaldehyde oxidation, as well as partial oxidation of cyclohexane over metal oxides allowed us to detect all the radical intermediates that are expected for these reactions. Therefore, we believe this method can be useful for mechanistic studies of gas phase reactions, particularly those focused on the role of peroxides over metal surfaces and it can provide better results than current methodologies such as matrix isolation for the trapping of gas phase species. We think our findings can possibly be extended to atmospheric chemistry or tobacco industry, as well as further catalytic reactions in gas phase such as photochemical reactions[50] or hydrocarbons aromatization processes.[51] This method could help establish if some important industrial processes such as maleic anhydride synthesis over metal phosphorous oxides[52] occur via radical pathway,[53] with clear repercussion for the catalyst design. Further development of the reactor could involve the use of different materials for the walls, in order to discriminate any possible effect of quenching of the radicals to the walls and to increase sensitivity.

ACKNOWLEDGMENTS

Funding for this work was provided by the EPSRC (Grant No. EP/E001629/1) and Research Support and Priming Fund Grant by the Department of Chemistry of the University of York (Grant No. P0008503). The authors thank Mr. Chris Mortimer of the mechanical workshop of the Chemistry department at the University of York for the assembling of the reactor and the design of the cooling system and Gareth Moody for GC determinations.

[1] P. S. Monks, Chem. Soc. Rev. **34**, 376 (2005).
[2] A. H. Laufer and A. Fahr, Chem. Rev. (Washington D. C.) **104**, 2813 (2004).
[3] A. Baiker, Chem. Rev. (Washington, D. C.) **99**, 453 (1999).
[4] *Electron Paramagnetic Resonance: A Practitioners' Toolkit*, edited by M. Brustolon and E. Giamello (Wiley, Hoboken, 2009).
[5] A. Weil, J. R. Bolton, and J. E. Wertz, *Electron Paramagnetic Resonance* (Wiley, New York, 1994).
[6] L. Andrews, Annu. Rev. Phys. Chem. **22**, 109 (1971).
[7] D. F. Church, Anal. Chem. **66**, 419A (1994).
[8] D. Mihelcic, D. H. Ehhalt, G. F. Kulessa, J. Klomfass, M. Trainer, U. Schmidt, and H. Röhrs, Pure Appl. Geophys. **116**, 530 (1978).
[9] J. A. Howard, R. Jones, J. S. Tse, M. Tomietto, P. L. Timms, and A. J. Seeley, J. Phys. Chem. **96**, 9148 (1992).
[10] R. P. Mason, P. M. Hanna, M. J. Burkitt, and M. B. Kadiiska, Environ. Health Perspect. **102**, 33 (1994).
[11] P. Ionita, M. Conte, B. C. Gilbert, and V. Chechik, Org. Biomol. Chem. **5**, 3504 (2007).
[12] M. Conte, K. Wilson, and V. Chechik, Org. Biomol. Chem. **7**, 1361 (2009).

[13] M. Conte, H. Miyamura, S. Kobayashi, and V. Chechik, J. Am. Chem. Soc. **131**, 7189 (2009).
[14] M. Conte, H. Miyamura, S. Kobayashi, and V. Chechik, Chem. Commun. (Cambridge) **2010**, 145.
[15] Z. Maskos, L. Khachatryan, R. Cueto, W. A. Pryor, and B. Dellinger, Energy Fuels **19**, 791 (2005).
[16] W. A. Pryor, M. Tamura, and D. F. Church, J. Am. Chem. Soc. **106**, 5073 (1984).
[17] J. D. Honeywill and B. Mile, Magn. Reson. Chem. **38**, 423 (2000).
[18] A. Corma and H. García, Chem. Rev. (Washington, D. C.) **102**, 3837 (2002).
[19] J. G. Speight, *Chemical and Process Design Handbook* (McGraw-Hill, New York, 2002).
[20] See http://epr.niehs.nih.gov/pest.html for the WINSIM software.
[21] F. W. Barlow, *Rubber Compounding: Principles, Materials, and Techniques*, 2nd ed. (Dekker, New York, 1993).
[22] E. Niki, Y. Kamiya, and N. Ohta, Bull. Chem. Soc. Jpn. **41**, 1466 (1968).
[23] A. G. Janzen and B. J. Blackburn, J. Am. Chem. Soc. **91**, 4481 (1969).
[24] S. L. Baum, I. G. M. Anderson, R. R. Baker, D. M. Murphy, and C. C. Rowlands, Anal. Chim. Acta **481**, 1 (2003).
[25] M. J. Davies and T. F. Slater, Biochem. J. **240**, 789 (1986).
[26] D. L. Haire, U. M. Oehler, P. H. Krygsman, and E. G. Janzen, J. Org. Chem. **53**, 4535 (1988).
[27] M. J. S. Gynane, M. F. Lappert, P. I. Riley, P. Rivière, and M. Rivière-Baudet, J. Org. Chem. **202**, 5 (1980).
[28] M. Conte, Y. Ma, C. Loyns, P. Price, D. Rippon, and V. Chechik, Org. Biomol. Chem. **7**, 2685 (2009).
[29] *Reactive Intermediate Chemistry*, edited by R. A. Moss, M. S. Platz, and M. Jones (Wiley, New York, 2004).
[30] G. Zhou, B. Zhao, J. Hou, M. Li, C. Chen, and W. Xin, Biotechnol. Tech. **13**, 507 (1999).
[31] R. A. Sheldon and J. K. Kochi, *Metal-Catalyzed Oxidations of Organic Compounds* (Academic, New York, 1981).
[32] *Liquid Phase Oxidation, Comprehensive Chemical Kinetics 16*, edited by B. H. Bamford and C. F. H. Tipper (Elsevier, Amsterdam, 1980).
[33] E. G. Janzen, E. R. Davis, and C. M. DuBoset, Magn. Reson. Chem. **33**, S166 (1995).
[34] N. Ohto, E. Niki, and Y. Kamiya, J. Chem. Soc., Perkin Trans. 2 1770 (1977).
[35] S. Bhaduri and D. Mukesh, *Homogeneous Catalysis: Mechanisms and Industrial Applications* (Wiley, New York, 2000).
[36] G. Centi, F. Cavani, and F. Trifirò, *Selective Oxidation by Heterogenous Catalysts* (Academic, New York, 2001).
[37] J. D. Holladay, Y. Wang, and E. Jones, Chem. Rev. (Washington, D. C.) **104**, 4767 (2004).
[38] The unusually low hydrogen coupling constant for this spin adduct cannot be assigned to an alternative DMPO spin adduct such as carbon, oxygen, or hydrogen-centred radicals, and it is likely to be an oxidation product similar to DMPOX which has $a_H < 5$ G. However the presence of this species does not affect our conclusions.
[39] B. Kalyanaraman, C. Mottley, and R. P. Mason, J. Biochem. Biophys. Methods **9**, 27 (1984).
[40] E. J. Silke, W. J. Pitz, C. K. Westbrook, and M. Ribaucour, J. Phys. Chem. A **111**, 3761 (2007).
[41] E. G. Janzen, C. A. Evans, and J.-P. Liu, J. Magn. Reson. **9**, 513 (1973).
[42] V. Govindan and A. K. Suresh, Ind. Eng. Chem. Res. **46**, 6891 (2007).
[43] A. Bhattacharya and A. Mungikar, Can. J. Chem. Eng. **81**, 220 (2003).
[44] M. A. Rudat and C. N. McEwen, J. Am. Chem. Soc. **103**, 4349 (1981).
[45] J. L. G. Fierro, *Metal Oxides: Chemistry and Applications* (Taylor & Francis, Boca Raton, 2006).
[46] T. Ressler, A. Walter, Z.-D. Huang, and W. Bensch, J. Catal. **254**, 170 (2008).
[47] M. Gillet, K. Aguira, C. Lemirea, E. Gilleta, and K. Schierbaumb, Thin Solid Films **467**, 239 (2004).
[48] L. Dall'Acqua, I. Nova, L. Lietti, G. Ramis, G. Buscac, and E. Giamello, Phys. Chem. Chem. Phys. **2**, 4991 (2000).
[49] G. Mestl, N. F. D. Verbruggen, E. Bosch, and H. Knözinger, Langmuir **12**, 2962 (1996).
[50] N. Hoffmann, Chem. Rev. (Washington, D. C.) **108**, 1052 (2008).
[51] A. Corma, Chem. Rev. (Washington, D. C.) **97**, 2373 (1997).
[52] M. Conte, G. Budroni, J. K. Bartley, S. H. Taylor, A. F. Carley, A. Schmidt, D. M. Murphy, F. Girgsdies, T. Ressler, R. Schlögl, and G. J. Hutchings, Science **313**, 1270 (2006).
[53] N. Dietl, M. Engeser, and H. Schwarz, Angew. Chem., Int. Ed. **48**, 4861 (2009).